

Classification of reflectors with an ultrasonic sensor for mobile robot applications

Jesús Ureña *, Manuel Mazo, J. Jesús García, Álvaro Hernández, Emilio Bueno

*Department of Electronics, University of Alcalá, Escuela Politécnica, Campus Universitario s/n,
28 805 Alcalá de Henares, Madrid, Spain*

Received 9 October 1998; received in revised form 21 March 1999; accepted 12 May 1999

Communicated by F.C.A. Groen

Abstract

This paper describes a sensor model made up of four ultrasonic transducers able to classify reflectors (wall, edge or corner) in specular environments. The main goal has been to effect the classification from a single reading cycle: emission of ultrasounds and reception of echoes (measuring only times of flight—TOFs). Working from the four TOFs obtained after a single emission of ultrasounds (thereby facilitating its practical implementation in a mobile robot, when readings are taken while the robot is moving), an algorithm has been proposed for discriminating between edge and plane type reflectors. The configuration of the four transducers enabled dependent discriminating functions to be determined directly from the quadratic terms of the TOFs, without the need for previous geometric transformations. Special attention was given to the effect of the separation between the sensor transducers and the reading-associated noise. Finally, some considerations have been pointed out about the possibility of two transducers emitting, so allowing discrimination between walls and corners. ©1999 Published by Elsevier Science B.V. All rights reserved.

Keywords: Ultrasonic sensor; Intelligent sensor; Mobile robot; Reflector discrimination

1. Introduction

One of the main goals when using multi-transducer ultrasonic sensors is to be able to discriminate the sort of object from which the echo signal has been reflected. In practice, in specular environments a three reflector type classification has become the norm [1,4]: plane, edge and corner. The plane is reserved for reflectors such as walls or similar smooth surfaces, while the edge represents rounded or convex objects. The

corner is a concave reflector (normally two planes intersecting at right angles).

In terms of mobile robots the advantages of gaining information of the reflector type may be important in given applications, such as

- In the identification of certain objects that may constitute guidance objectives (such as the tracking of planes, for example) or for the positioning of the mobile robot within an environment (such as the localisation of certain pre-established marks).
- In map building of the mobile robot's environment a knowledge of the reflector type entails an added advantage (for example in the adequate updating of grids with certainty values).

* Corresponding author. Tel.: +34-918856544-40;
fax: +34-918856591.

E-mail address: urena@depeca.alcala.es (J. Ureña)

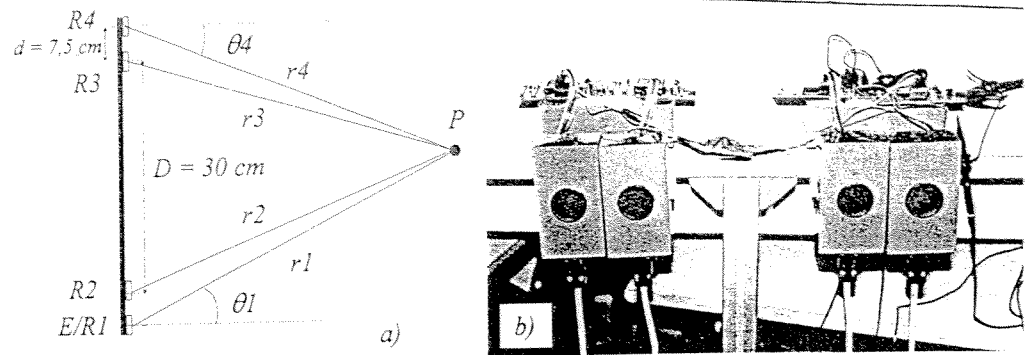


Fig. 1. (a) Basic sensor structure with four transducers; and (b) image of a prototype.

For the identification of this type of reflectors, working from times of flight (TOF), an active perception of the environment is needed (i.e., different “points of view”). This is done either by exploiting the successive readings as the mobile moves along, or by using more than one ultrasound receptor for each emitter [4,5]. As has been shown in [2] at least two emitters suitably separated are required for the classification of the three types of reflectors (planes, corners and edges), and the pulses of these emitters must also be received by at least two receivers. If there have to be two emitters, and these must not emit simultaneously, the identification data will not be obtained in a given instant of time but rather after at least two reading periods. In mobile robots this raises problems, not only in terms of the time taken to gain both readings but also because it is necessary to know the robot’s positioning [3].

When readings are taken from different points with a view to detecting the same reflector, there are added problems in the precise determination of the position of the mobile robot (normally obtained from odometric systems). Moreover, when several readings are being processed (either taken simultaneously by several transducers or by a single transducer from different points) it is necessary to determine whether or not the echoes detected have come from the same reflector (an echo correspondence problem) [4]. The maximum differences that may exist between readings may at least be established geometrically, to achieve correspondence [2].

A description is given below of the configuration of the proposed sensor (Section 2), plus the classifica-

tion algorithm, at first to discriminate between edges and other reflectors (Section 3). Then, in Section 4, attention is turned to the adaptation of the sensor to the considerations for the discrimination between planes and corners. Lastly in Section 5, the most important conclusions are given.

2. Basic sensor

The basic sensor system proposed, which has been tried out in different situations, consists of four transducers separated as shown in Fig. 1a and b. The transducers work at 50 kHz and have an aperture angle of 30° . Each transducer has been improved to a good precision in distance measurements (error lower than 2 mm in distances up to 2 m) [6]. When transducer E/R1 is emitting, from that moment on all transducers are waiting for the echo, thereafter processing and determining the TOF for each one of them.

In general, a pair of receivers can give, as well as the reflector distance, the angle of arrival [2]. The problem of correspondence (determining whether both receivers have detected the same object) is minimized by placing them as close together as possible. In the system proposed here, in order to measure the angle of arrival on both ends of the sensor, there are two pairs of receivers separated by only 7.5 cm (the diameter of the transducer employed is 4 cm).

In general, for a pair of transducers, where one of the two receivers is also an emitter (E/R1), the ambiguity area (the space wherein the different reflectors can

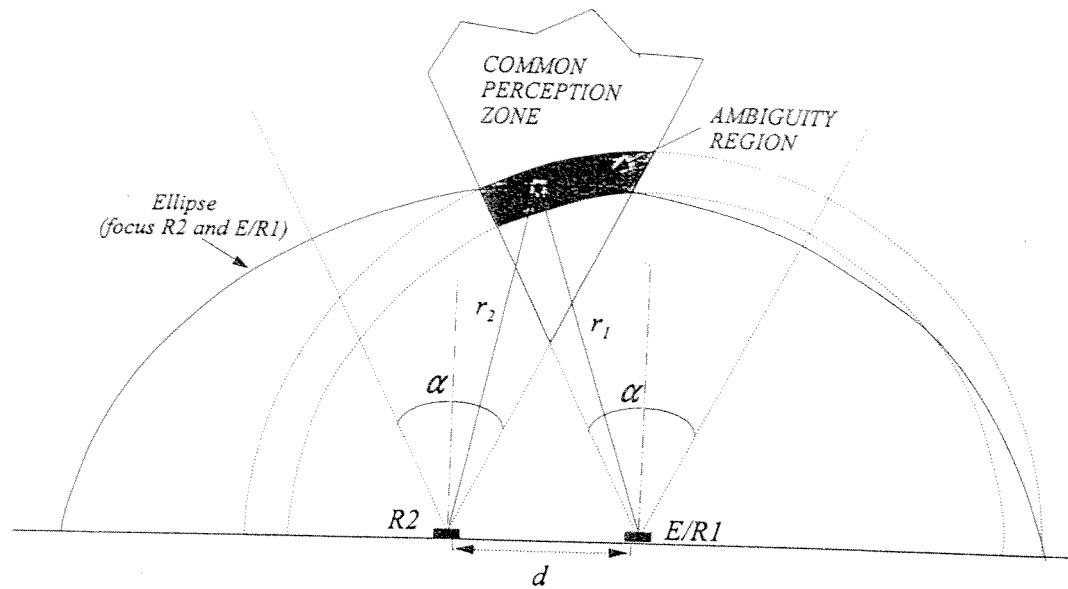


Fig. 2. Ambiguity region for two receptors (when one emit).

not be discriminated) corresponds to the shaded zone shown in Fig. 2. This area is determined mainly by the apertures of the emission/reception patterns of the transducers (total angle) and the separation between both receivers (d).

If R2 has measured a TOF, t_2 , the reflector detected may have been in any of the ellipse points shown in Fig. 2, with foci in both receivers. For a point of the said ellipse, which is at a distance r_1 from transducer T/R1 and at a distance r_2 from R2, the following will hold:

$$r_1 + r_2 = c \cdot t_2, \quad (1)$$

where " c " is the speed of the ultrasounds in the air. If the reflector is in a perception zone common to both receivers, receiver E/R1 will detect a TOF that may vary in accordance with the precise position occupied by the reflector on the aforementioned ellipse and within the common zone. For E/R1, therefore, the reflector can be seen as it will be between the two concentric circumferences shown in Fig. 2. It may then be demonstrated geometrically that, if $c \cdot t_2 \gg d \cdot \sin(\alpha/2)$, the time of flight detected by R1 (t_1) should by all rights be included between the values given by the following equation:

$$\begin{aligned} t_2 - \frac{d}{c} \cdot \sin \frac{\alpha}{2} &\leq t_1 \leq t_2 + \frac{d}{c} \cdot \sin \frac{\alpha}{2}, \\ |t_2 - t_1| &\leq \frac{d}{2} \cdot \sin \frac{\alpha}{2}. \end{aligned} \quad (2)$$

The above equation can then be used to determine whether or not there is correspondence between the TOFs detected by each pair of transducers.

When two receivers are separated by a distance d , there would be an important "dead" zone between both receivers, where obstacles would not be detected. It immediately follows that the minimum distance measured by any of the two receivers (if both have detected the same reflector) must be greater than $(d/2)/(\sin \alpha/2)$.

3. Discrimination between edges and planes

3.1. Readings for edges and planes

The sensor has been modelled on the assumption that, after the reflection, the ultrasound signals arrive at the receivers as though they had been emitted from a point P. In the case of an edge-type reflector this point coincides with the physical position of the same;

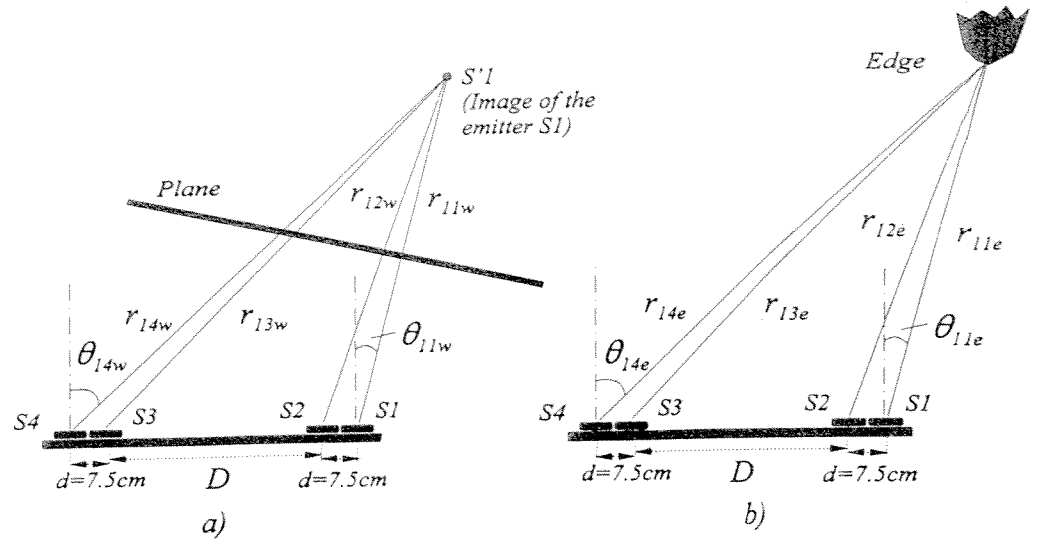


Fig. 3. Distances and angles for (a) plane and (b) edge reflectors.

in the case of walls and corners it is a point of the image plane.

The situation for both types of reflectors (edges and planes) can be seen in Fig. 3. The nomenclature adopted uses a triple subscript, the first showing the transducer that is emitting; the second, the transducer receiving and the third, the type of reflector ("e" for edges and "w" for walls or planes). Note that the geometric relations between the situations presented in Fig. 3a and b are identical. The difference lies in the method of obtaining distances from the TOFs that have been measured. Hence we get the following:

$$\begin{aligned} r_{1je} &= c \cdot \left(t_{1j} - \frac{t_{11}}{2} \right), \quad j = 1, 2, 3, 4, \\ r_{1jw} &= c \cdot t_{1j}, \quad j = 1, 2, 3, 4, \end{aligned} \quad (3)$$

where r_{1je} and r_{1jw} are the distances for both reflector types, t_{1j} is the TOF detected by the receiver "j" when it has emitted the transducer "1" (in this study S1 is the emitter) and c is the speed of the ultrasound in air.

3.2. Case of readings without noise

For both diagrams in Fig. 3 the following relation can be obtained between the measured distances and the geometry of the sensor:

$$r_{14}^2 + r_{11}^2 - r_{13}^2 - r_{12}^2 = 2d \cdot (D + d), \quad (4)$$

and using (3) for every type of reflector:

$$\begin{aligned} \text{Wall : } \frac{2d \cdot (D + d)}{c^2} &= K \\ &= t_{14}^2 + t_{11}^2 - t_{13}^2 - t_{12}^2 = f_{\text{wall}}, \\ \text{Edge : } \frac{2d \cdot (D + d)}{c^2} &= K \\ &= t_{14}^2 - t_{13}^2 - t_{12}^2 + t_{11}(t_{12} + t_{13} - t_{14}) = f_{\text{edge}} \end{aligned} \quad (5)$$

The value $K = 2d(D + d)/c^2$ is a constant reference (in s^2) depending on the sensor structure (d and D) and the velocity of the ultrasound in the air (c). Once a measurement has been taken, the TOFs can be used to obtain the functions f_{wall} and f_{edge} defined as it is indicated in (5). With the supposition of no noise in the measurements these expressions can be used directly to determine the reflector type, because

$$\text{If } f_{\text{wall}} - K = 0 \Rightarrow \text{Wall},$$

$$\text{If } f_{\text{edge}} - K = 0 \Rightarrow \text{Edge}.$$

3.3. Case of readings with noise

For every transducer the noise can be modeled as a zero-mean gaussian with standard deviation σ [4]. After the emission of an ultrasound pulse with S1 and

the reception in S1, S2, S3 and S4, there is a vector of TOFs (\mathbf{T}) given by

$$\mathbf{T} = [t_{11}, t_{12}, t_{13}, t_{14}] = \mathbf{t} + \mathbf{n}_u + \mathbf{n}_c, \quad (7)$$

where \mathbf{t} is the vector of actual TOFs and \mathbf{n}_u and \mathbf{n}_c are two independent vectors (with the same dimension of \mathbf{t}) that represent the transducer noise components (zero-mean) uncorrelated (σ_u) and correlated (σ_c), respectively. Then $\sigma^2 = \sigma_c^2 + \sigma_u^2$.

If Σ^{tot} is the covariance matrix of \mathbf{T} and \mathbf{J} is the Jacobean of the transformation of \mathbf{T} in the vector ($f_{\text{wall}}, f_{\text{edge}}$)—in accordance with (5)—, the covariance matrix of the last vector will be

$$\text{cov}(f_{\text{wall}}, f_{\text{edge}}) = \begin{pmatrix} \sigma_{ww}^2 & \sigma_{we}^2 \\ \sigma_{we}^2 & \sigma_{ee}^2 \end{pmatrix} = \mathbf{J} \cdot \Sigma^{\text{tot}} \cdot \mathbf{J}' \quad (8)$$

From this Eq. (8) and with the approximations $t_A = t_{11} \simeq t_{12}$ and $t_B = t_{14} \simeq t_{13}$ (well justified after geometric considerations):

$$\begin{aligned} \sigma_{ww}^2 &= 8 \cdot \sigma_u^2 \cdot [t_A^2 + t_B^2], \\ \sigma_{ee}^2 &= 4 \cdot \sigma_u^2 \cdot [(t_A - t_B)^2 + t_B^2], \\ \sigma_{we}^2 &= 4 \cdot \sigma_u^2 \cdot [t_A^2 - t_A t_B + 2t_B^2]. \end{aligned} \quad (9)$$

It is important to establish the fact that only the uncorrelated component of the noise present in the transducers (σ_u) has an influence in the covariance matrix of ($f_{\text{wall}}, f_{\text{edge}}$). This has an important practical consideration because it means that the noise present in all the transducers has a little influence on the discrimination functions. This is the case, for example, of the environmental changes (i.e. the room temperature) that has a similar influence on all transducers.

The standard deviation of f_{wall} and f_{edge} can be approximately obtained from (9) knowing σ_u (from empirical test it has been assumed a value of $4 \mu\text{s}$ —measured when the reflector is 1 m apart). These standard deviations rise with the TOFs. Furthermore, σ_{ww}^2 can be up to four times greater than σ_{ee}^2 . The average values for ($f_{\text{wall}}, f_{\text{edge}}$) are ($2K, K$) for edges and ($K, K/2$) for planes, where K is the value defined in (5).

3.4. Classification algorithm

The correlation between f_{wall} and f_{edge} , high for long TOFs, calls for using a classification algorithm

where both functions are employed in an independent way. Fig. 4 shows the flow chart followed for the discrimination between edges and walls. First, the correspondence between echoes is determined (if there are no jumps between two TOFs greater than $(d/c) \sin(\alpha/2)$, where d is the separation between transducers and α their aperture angle).

When there is no correlation of echoes only distances and sometimes angles can be determined. On the other hand, if there is correspondence of echoes the classification algorithm can perform the following operations: calculating f_{wall} and f_{edge} , σ_{ww} and σ_{ee} , and assigning a type of reflector according to the following expressions (in a first approximation):

$$\begin{aligned} \text{Edge: } f_{\text{edge}} &\geq \frac{3K}{4} \quad \text{or} \quad f_{\text{wall}} \geq \frac{3K}{2}, \\ \text{Plane: } f_{\text{edge}} &< \frac{3K}{4} \quad \text{or} \quad f_{\text{wall}} < \frac{3K}{2}. \end{aligned} \quad (10)$$

Once the discrimination has been effected according to the above parameters, the definitive assignment to one of the classes is effected only if the evaluated probability function comes within a set interval around the average, that is:

$$\begin{aligned} P(f_{\text{edge}}|\text{edge}) &= \frac{1}{\sqrt{2\pi}\sigma_{ee}} \cdot e^{-(f_{\text{edge}}-K)^2/2\sigma_{ee}^2} \\ &\Rightarrow \text{Edge} \quad \text{if } f_{\text{edge}} \in [K \pm 2\sigma_{ee}], \\ P(f_{\text{wall}}|\text{wall}) &= \frac{1}{\sqrt{2\pi}\sigma_{ww}} \cdot e^{-(f_{\text{wall}}-K)^2/2\sigma_{ww}^2} \\ &\Rightarrow \text{Wall} \quad \text{if } f_{\text{wall}} \in [K \pm 2\sigma_{ww}], \end{aligned} \quad (11)$$

where $P(f_{\text{edge}}|\text{edge})$ is the probability of having an edge for a given value of f_{edge} and $P(f_{\text{wall}}|\text{wall})$ is the probability of having a wall for a given value of f_{wall} .

3.5. Results

This algorithm has been tested with data from a simulator with a different degree of noise coupled to the data. The goal of these simulations was to test the influence of the noise in f_{wall} and f_{edge} then it has been supposed that there is no correspondence problem.

Results from the simulator prove the validity of the method, if the reading error has a typical deviation of less than 2 mm and the sensor length is 30 cm or more. This is demonstrated in Fig. 5, showing the values of f_{edge} , f_{wall} and K for 125 reading samples taken

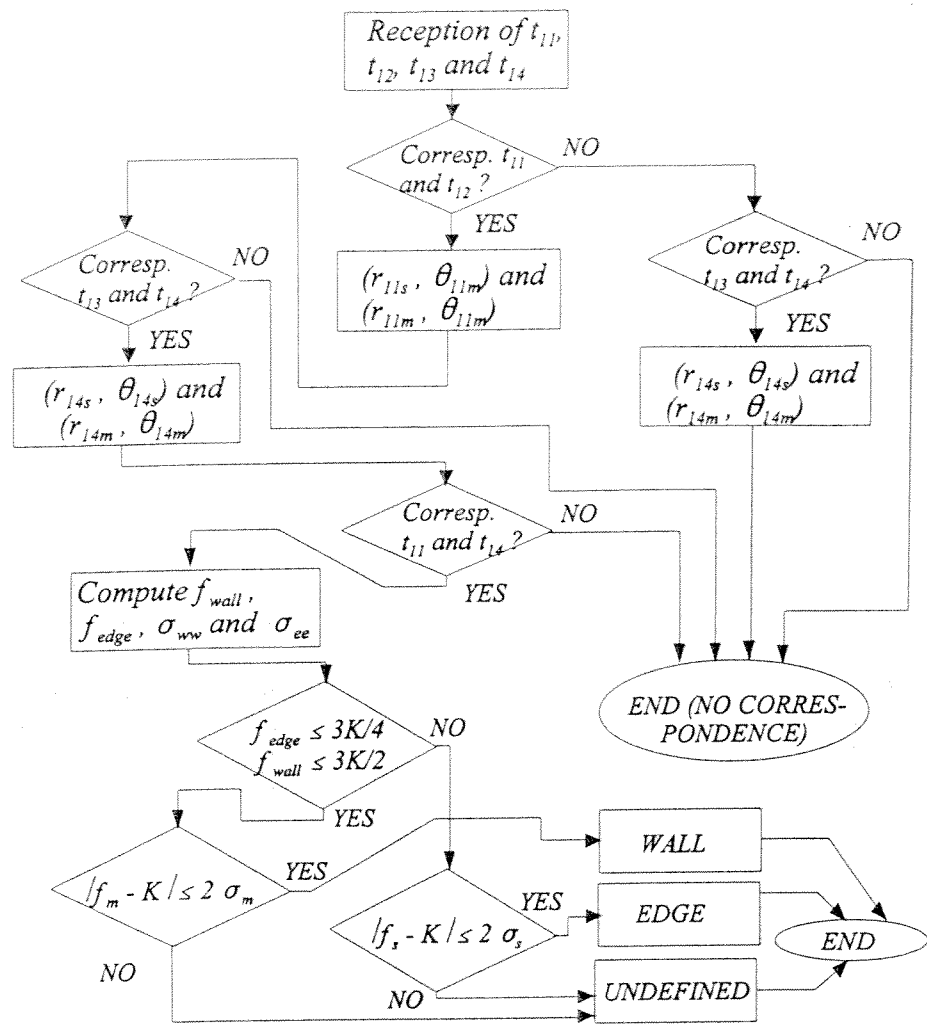


Fig. 4. Flow-chart for the classification algorithm (edges and planes).

with the sensor up against a plane reflector at 150 cm, with inclinations varying from -15° to $+15^\circ$. These readings have been contaminated with a gaussian noise with a typical deviation of 1 mm. Results are shown for three sensor lengths (D): 10, 30 and 50 cm. It should be noted that, in this case, the values of f_{wall} are all in the vicinity of K while the values of f_{edge} are all around the value $K/2$. The greater is D , the easier is the discrimination.

Fig. 6 shows a representation similar to that of Fig. 5 but now for 252 data samples obtained in each case

from placing an edge type reflector in front of the sensor, at a distance of about 150 cm and with deviation from its main axis ranging from -80 to $+80$ cm. In this case it is the variable f_{edge} that takes on a value similar to that of K , while f_{wall} is in the vicinity of $K/2$. The discrimination is again easier with higher values of D .

The algorithm has also been tested with real readings obtained with the sensor set against a reflector placed in known positions. In this case, obviously, the problem of correspondence has been considered, the

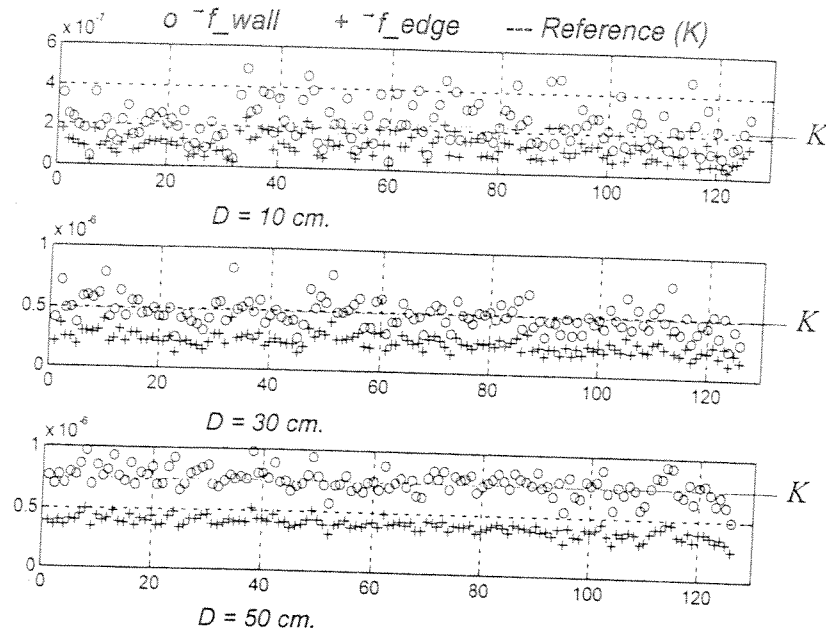


Fig. 5. Results of simulation: values of f_{edge} , f_{wall} and K for plane-type reflectors (at a distance of 150 cm with $\sigma = 1$ mm).

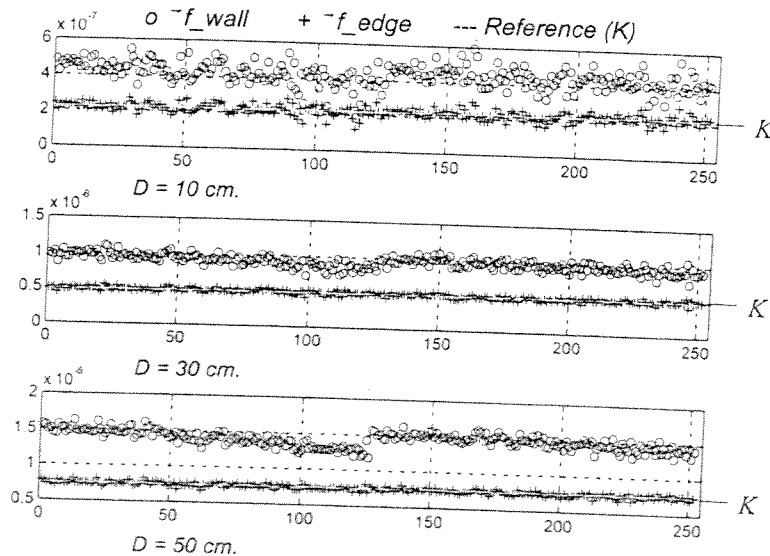


Fig. 6. Results of simulations: values of f_{edge} , f_{wall} and K for edge-type reflectors (at a distance of 150 cm and with $\sigma = 1$ mm).

there are more different possibilities of results than the simulated case. For edge type reflectors a 9 cm diameter PVC cylinder was used and for plane type reflectors a polywood board 144 cm high and 288 cm wide was used. These readings were used for determining the influence on the algorithm of the position (and in-

clination in the case of planes) of the reflector and the total sensor length. A sensor length of $D = 30$ cm was thereby chosen, as a compromise between the discrimination capacity of the sensor, the acceptable level of error in the readings and the location of the reflector in the front zone of the sensor.

Table 1

Results of the classifier with 200 samples of real data when the reflector is plane type (x is the distance from the reflector to the sensor and θ_{inc} is the angle of inclination of the plane)

Position	No correspondence	Correspondence only on one side	Correspondence in A and B	Wall	Edge	Indetermination
$x = 150$ cm	0	0	0	121	11	68
$\theta_{inc} = 0^\circ$	(0%)	(0%)	(0%)	(60.5%)	(5.5%)	(34%)
$x = 150$ cm	0	5	0	99	21	75
$\theta_{inc} = -10^\circ$	(0%)	(2.5%)	(0%)	(49.5%)	(10.5%)	(37.5%)
$x = 150$ cm	0	3	0	105	16	76
$\theta_{inc} = 10^\circ$	(0%)	(1.5%)	(0%)	(52.5%)	(8%)	(38%)

Table 2

Results of classifier with 200 samples of real data when the reflector is edge type (x is the distance from the reflector to the sensor and y is the separation of the reflector from the main axis of the sensor)

Position	No correspondence	Correspondence only on one side	Correspondence in A and B	Wall	Edge	Indetermination
$x = 100$ cm	1	0	0	3	192	4
$y = 0$ cm	(0.5 %)	(0%)	(0%)	(1.5%)	(96%)	(2%)
$x = 100$ cm	0	65	0	8	119	8
$y = -10$ cm	(0%)	(32.5%)	(0%)	(4%)	(59.5%)	(4%)
$x = 100$ cm	0	64	0	6	123	7
$y = 10$ cm	(0%)	(32%)	(0%)	(3%)	(61.5%)	(3.5%)
$x = 185$ cm	2	22	2	32	116	26
$y = 0$ cm	(1%)	(11%)	(1%)	(16%)	(58%)	(13%)
$x = 185$ cm	2	67	3	28	84	16
$y = -20$ cm	(1%)	(33.5%)	(1.5%)	(14%)	(42%)	(8%)
$x = 185$ cm	4	70	2	24	80	20
$y = 20$ cm	(2%)	(35%)	(1%)	(12%)	(40%)	(10%)

The results of the classifier, with real data (200 readings samples in each position), when a plane or edge type reflector is placed in front of the sensor are shown in Tables 1 and 2, respectively. In both cases " x " is the distance from the reflector. For planes, θ_{inc} is given as the inclination angle and for edges " y " is given as the separation from the sensor's main axis. In both cases the classification percentages obtained are shown, including the cases in which the algorithm could not be completed due to correspondence problems (as shown in the diagram of Fig. 4).

It should be noted that these correspondence problems arise above all in the case of edges significantly offset from the sensor's main axis; in this case, logically, one side of the sensor captures the reflector better than the other. They also arise in the case of a plane reflector if it has a significant inclination. These factors, together with great distances from the sensor to

the reflector (more than about 2 m), have a considerable adverse effect on the classifier's results.

4. Plane-corner case consideration

From a theoretical point of view, a corner-type reflector (on the assumption of a specular relation) can be modeled with a double reflection according to the set-up shown in Fig. 7b. The corresponding reflection of Fig. 7a, for a plane, and 7b, for a corner, show that the final image of the transducer S1 falls in both cases in the same place (point P in both figures). The distances and angles obtained after the emission of sensor S1 would then be the same in both cases.

If the emission were made with S4, then there would be a difference; nonetheless a position of the corner could be found that represents a situation

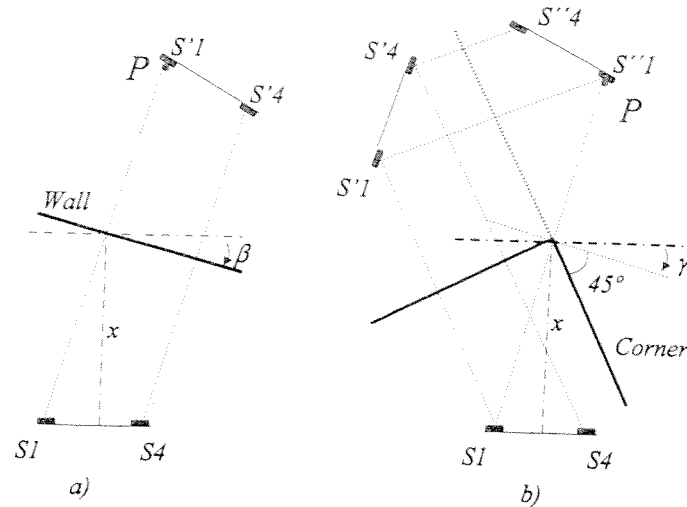


Fig. 7. Specular image of a sensor: (a) for a plane and (b) for a corner.

ambiguity similar to that previously shown for S1. On the assumption that readings are obtained after emissions of S1 and S4 then, a discrimination function can be deduced geometrically, which function can then be used in the final classification between “planes” and “corners”. The procedure could be as follows:

- Take readings when S1 has emitted and determine whether the reflector corresponds to a plane or an edge. Carry out separately an identical operation for readings obtained when S4 has emitted.
- If, after the above procedure, both should have detected a plane type reflector, carry out a new classification.

To this end, a discrimination function could be: $f_{disc} = \theta_{44} - \theta_{11}$, where θ_{44} is the angle detected by transducer 4 when this transducer is emitting and θ_{11} is the angle detected by transducer 1 when this transducer is emitting. It should be noted that in the case of a wall this function would be zero while in the case of a corner the following might hold:

$$\tan \theta_{44} - \tan \theta_{11} = \frac{D + 2d}{x} \quad (12)$$

Furthermore, given that the angles detected will always be sufficiently small, the above equation can be approximated, with the following definitive result:

$$\begin{aligned} f_{disc} &= \theta_{44} - \theta_{11} = \frac{D + 2d}{x} \quad \text{if corner,} \\ f_{disc} &= \theta_{44} - \theta_{11} = 0 \quad \text{if plane.} \end{aligned} \quad (13)$$

Note that, according to the above equation, the discrimination depends on the sensor dimensions ($D+2d$): the greater the separation between transducers, the better the results (albeit with the offsetting disadvantage of the separation of the sensors’ “perspectives” and a heightening of the problems bound up with echo correspondence). Discrimination is also better with short distances (values less of “ x ”) than with long distances.

5. Conclusions

This paper has described an ultrasonic sensor model made up by four transducers. Exploiting the geometric behaviour, and on the assumption of specular reflections, an algorithm has been proposed for discriminating between different reflector types.

Working from the four TOFs obtained after a single emission of ultrasounds (thereby facilitating its practical implementation in a mobile robot, when readings are taken while the robot is moving), an algorithm has been proposed for discriminating between edge and plane type reflectors. The configuration of the four transducers enabled dependent discriminating

functions to be determined directly from the quadratic terms of the TOFs, without the need for previous geometric transformations (such transformations are necessary in the case of algorithms proposed for other sensor set-ups [2,4]), which require certain trigonometric relations after the transformation of the TOFs into distances. The sensor's capacity for discriminating between reflectors has been shown, in terms of a characteristic parameter depending on its geometry (K), including the distance between the end transducers (d) and the separation between end pairs (D).

The influence of noise on the discrimination functions has also been studied, the conclusion being drawn that only the uncorrelated component of noise in the different transducers has an effect, but not the correlated component (i.e., the noise motivated by environmental factors that has effect on all transducers has no influence). To consider the influence of noise a statistic classifier has been set up, wherein the typical deviation of the functions used is obtained from the typical error deviation of a single transducer and the TOF readings. The proposed algorithm has been tested with simulated data to which different noise levels were added, and also with real data. Results show the great influence of the sensor's K parameter (the greater the separation between transducers, the greater the discrimination possibility, but at the cost of greater echo-correspondence problems). It has also been shown that the classification falls off, with equal noise levels, as the TOF readings increase.

In any case, the transducers must be capable of making readings with millimetric precision. Thus, there is a fairly close relationship between the results obtained with real data coming from the sensor and the reading errors. It has been shown that the typical noise deviation is less than 2 mm in the measurement of distances up to about 2 m in the case of edges and up to 3 m in the case of planes. Even below these distances the classifier results are also determined by the imperfections of the reflectors, the geometric tolerances of the sensor and the different behaviour of the various transducers.

If the result of the classifier is a plane, then a second reading (taken from the other end of the sensor) can be used to determine geometrically whether it really is a plane or a corner. All cases presented, in terms of the readings taken and the sensor's possibilities, should be tested by higher level algorithms (mapping, posi-

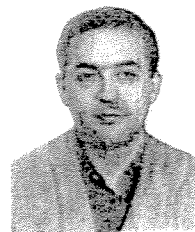
tioning, etc.). Note that in real environments situations may arise of non-correspondence between transducers or non-classification of reflector type. It should also be noted that even though the classification algorithm is effective only over short and intermediate distances, distance readings over greater ranges are also available, and these can be taken into account for other considerations than those of classification.

Acknowledgements

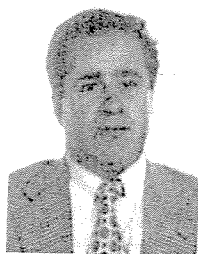
This work has been supported by the CICYT (Interministerial Commission of Science and Technology, Spain) projects TAP94-0656-C03-01 and TER96-1957-C03-01.

References

- [1] Ö. Bozma, R. Kuc, Characterizing pulses reflected from rough surfaces using ultrasounds, *J. Acoust. Soc. Amer.* 6 (1999) 2519–2531.
- [2] L. Kleeman, R. Kuc, Mobile robot sonar for target localization and classification, *Int. J. Robotics Res.* 14 (4) (1997) 295–318.
- [3] J. Leonard, H. Durrant-White, Mobile robot localization tracking geometric beacons, *IEEE Trans. Robotics Autom.* (3) (1991) 376–382.
- [4] H. Peremans, K. Audenaert, J.M. Van Campenhout, high-resolution sensor based on tri-aural perception, *IE Trans. Robotics Autom.* 9 (1) (1993) 36–48.
- [5] A.M. Sabatini, Active hearing for external imaging by means of an ultrasonic transducer array, *Proc. JROS'92*, Rayleigh, USA, 1992, pp. 829–836.
- [6] J. Ureña, M. Mazo, J.J. García, E. Bueno, A. Hernández, Low-cost improvement of an ultrasonic sensor and characterization for map-building, *ICV'98 (IFAC Workshop on Intelligent Components for Vehicles)*, Sevilla, Spain, March 1998, pp. 333–338.



Jesús Ureña received the Electronic Engineering and Telecommunication Engineering degrees from Polytechnic University of Madrid (Spain) in 1986 and 1992, respectively; and the Ph.D. degree in Telecommunications from the University of Alcalá (Spain) in 1998. Since 1998 he is a lecturer at the Electronic Department of the University of Alcalá. In this period he has collaborated in several educational and research projects in the areas of electronic communication and electronic and sensorial systems for mobile robots.



Manuel Mazo received the Electronic Engineering degree in 1976, the Telecommunications Engineering degree in 1982, and the Ph.D. degree in Telecommunications in 1988, all from the Polytechnic University of Madrid (Spain). He is currently Professor in the Department of Electronics at the University of Alcalá. His area of research are multi-sensor (ultrasonic, infrared and artificial vision) integration and electronic control systems applied to mobile robots and wheelchairs for physically disabled people.



Álvaro Hernández obtained his Telecommunication Engineering middle degree and Electronic Engineering degree from the University of Alcalá (Spain) in 1996 and 1998, respectively. Since 1998 he is a lecturer at the Electronic Department of the University of Alcalá. Currently, he is working for his Ph.D. His research areas are multi-sensor integration and electronic systems for mobile robots.



Juan Jesús García obtained his Electronic Engineering degree from the Polytechnical University of Alcalá de Henares, Spain, in 1992. He has been lecturer at the Electronic Department of the University of Alcalá since 1994. He has worked on several projects in relation to digital control, and his present areas of interest are mobile robots and multi-sensor integration.



Emilio José Bueno was born in Madrid, Spain, in October 31st, 1972. He got his middle degree in Telecommunication Engineering and Electronic Engineering at the University of Alcalá (Spain) in 1995 and 1999, respectively. His research areas are sensorless AC drives, FPGA-based control ICs for motor drives, DSP applications in power electronics and motion control. He is also researching into ultrasonic guidance of mobile robots.

**Journal Summary List**Journals from: **subject categories ROBOTICS & AUTOMATIC CONTROL**Sorted by: **Impact Factor****Sort Again**

Journals 1 - 20 (of 48)

|<<<[1|2|3]>>>|

Page 1 of 3

MARK ALL**UPDATE MARKED LIST***Ranking is based on your journal and sort selections.*

Mark	Rank	Abbreviated Journal Title (linked to journal information)	ISSN	Total Cites	Impact Factor	Immediacy Index	Articles	Cited Half-life
<input type="checkbox"/>	1	CHEMOMETR INTELL LAB	0169-7439	1381	1.657	0.328	125	5.3
<input type="checkbox"/>	2	IEEE T AUTOMAT CONTR	0018-9286	9163	1.643	0.095	304	9.6
<input type="checkbox"/>	3	SIAM J CONTROL OPTIM	0363-0129	2256	1.080	0.171	82	9.5
<input type="checkbox"/>	4	AUTON ROBOT	0929-5593	104	1.064	0.257	35	2.7
<input type="checkbox"/>	5	IEEE T ROBOTIC AUTOM	1042-296X	2133	0.984	0.321	109	7.6
<input type="checkbox"/>	6	IEEE-ASME T MECH	1083-4435	86	0.954	0.023	44	
<input type="checkbox"/>	7	AUTOMATICA	0005-1098	3802	0.911	0.152	191	7.3
<input type="checkbox"/>	8	SYST CONTROL LETT	0167-6911	1785	0.846	0.189	53	7.3
<input type="checkbox"/>	9	INT J ROBOT RES	0278-3649	1359	0.740	0.210	81	>10.0
<input type="checkbox"/>	10	IEEE CONTR SYST MAG	0272-1708	605	0.714	0.068	44	6.7
<input type="checkbox"/>	11	MATH CONTROL SIGNAL	0932-4194	409	0.676	0.067	15	9.5
<input type="checkbox"/>	12	J PROCESS CONTR	0959-1524	195	0.671	0.091	44	3.8
<input type="checkbox"/>	13	IEEE T SYST MAN CY B	1083-4419	297	0.665	0.042	96	3.2
<input type="checkbox"/>	14	IEEE T CONTR SYST T	1063-6536	246	0.562	0.029	69	3.6
<input type="checkbox"/>	15	INT J CONTROL	0020-7179	2674	0.530	0.084	143	>10.0
<input type="checkbox"/>	16	DISCRETE EVENT DYN S	0924-6703	78	0.483	0.000	16	
<input type="checkbox"/>	17	ROBOTICA	0263-5747	245	0.468	0.047	64	5.0
<input type="checkbox"/>	18	IEE P-CONTR THEOR AP	1350-2379	622	0.446	0.000	62	7.1
<input type="checkbox"/>	19	INT J ROBUST NONLIN	1049-8923	373	0.426	0.050	60	4.6
<input type="checkbox"/>	20	ROBOT AUTON SYST	0921-8890	183	0.415	0.014	72	3.8

MARK ALL**UPDATE MARKED LIST**

Journals 1 - 20 (of 48)

|<<<[1|2|3]>>>|

Page 1 of 3

Reprinted from

Robotics and Autonomous Systems

Robotics and Autonomous Systems 29 (1999) 269–279

Classification of reflectors with an ultrasonic sensor for mobile robot applications

Jesús Ureña *, Manuel Mazo, J. Jesús García, Álvaro Hernández, Emilio Bueno

*Department of Electronics, University of Alcalá, Escuela Politécnica, Campus Universitario s/n,
28 805 Alcalá de Henares, Madrid, Spain*

Received 9 October 1998; received in revised form 21 March 1999; accepted 12 May 1999

Communicated by F.C.A. Groen



Robotics and Autonomous Systems

*Host journal for the
Intelligent Autonomous Systems Society*

Editors-in-Chief:

Prof. F.C.A. Groen, University of Amsterdam, Faculty of Mathematics, Computer Science, Physics and Astronomy, Kruislaan 403, 1098 SJ Amsterdam, The Netherlands; E-mail: groen@wins.uva.nl

Prof. T.C. Henderson, University of Utah, Dept. of Computer Science, 3160, Merrill Engineering Building, Salt Lake City, UT 84112, USA; E-mail: tch@cs.utah.edu

Editorial Board

USA/Canada

J. ALBUS
Chair, Robot Systems Division
Nat. Inst. Standards and Technol.
Bldg. 220, Room B124
Gaithersburg
MD 20899, USA

CDR H.R. EVERETT Jr.
Naval Command Control &
Ocean Surveillance Center
RDT&E Division, Code 5303
San Diego, CA 92152-7381, USA

E. GRANT
ECE Department
North Carolina State University
Raleigh, NC 27695-7911, USA

R. GRUPEN
Department of Computer Science
Lederle Research Center
University of Massachusetts
Amherst, MA 01003, USA

W. GRUVER
Simon Fraser University
School of Engineering Science
Burnaby, BC, Canada V5A 1S6

S.A. HAYATI
Jet Propulsion Laboratory
4800 Oak Grove Drive
MS198-219
Pasadena, CA 91109, USA

A. KAK
Purdue University
School of Elect. Eng.
West Lafayette
IN 47907, USA

T. KANADE
Carnegie Mellon University
The Robotics Institute
5000 Forbes Avenue
Pittsburgh
PA 15213-3890, USA

D. NITZAN
Director of Robotics
Stanford Research Institute
333 Ravenswood Ave.
Menlo Park, CA 94025, USA

Europe

M. BOMAN
DSV
Electrum 230
SE 16440 Kista, Sweden

M. BRADY
University of Oxford
Dept. of Engineering Science
Parks Road
Oxford OX1 3PJ, UK

H. VAN BRUSSEL
Katholieke Universiteit Leuven
Dept. of Mechanical Engineering
Celestijnenlaan 300B
B-3001 Heverlee (Louvain), Belgium

J.L. CROWLEY
INRIA Rhone-Alpes
655 Avenue de l'Europe
38330 Montbonnot, France

R. DILLMAN
University of Karlsruhe
Institut für Prozessrechenstechnik
Automation und Robotik
Kaiserstrasse 12
D-76128 Karlsruhe
Germany

O.D. FAUGERAS
Computer Vision and Robotics Lab.
INRIA - SOPHIA
2004 route des Lucioles
06902 Valbonne Cedex
France

L.O. HERTZBERGER
University of Amsterdam
Dept. of Computer Systems
Kruislaan 403
1098 SJ Amsterdam
The Netherlands

G. HONDERD
Technische Universiteit Delft
Fac. der Electrotechniek
Mekelweg 4
2628 CD Delft
The Netherlands

C. MELCHIORRI
DEIS Università di Bologna
Via Risorgimento 2
40136 Bologna
Italy

H.-H. NAGEL
Fraunhofer-Institut für Informations-
und Datenverarbeitung (IITB)
Fraunhoferstr. 1
7500 Karlsruhe 1
Germany

J. SANTOS-VICTOR
Instituto Superior Tecnico
ISR - Torre Norte
Av. Rovisco Pais
1096 Lisboa Codex
Portugal

N. SHARKEY
University of Sheffield
Dept. of Computer Science
Regent Court
211 Portobello Street
Sheffield S1 4DP
UK

A. STEIGER GARÇAO
UNL FCT
Departamento de informática
Quinta da Torre
2825 Monte da Caparica
Portugal

W. VAN DE VELDE
Vrije Universiteit Brussels
A.I. Laboratory
Bldg. K, Floor 4
Pleinlaan 2
1050 Brussels
Belgium

Asia

T. FUKUDA
Department of Micro System
Engineering
Nagoya University
Furo-cho, Chikusa-ku
Nagoya, 464-01, Aichi, Japan

H. INOUE
University of Tokyo
Dept. of Mechano-Informatics
7-3-1 Hongo
Bunkyo-ku, Tokyo, Japan

H. MAKINO
Yamanashi University
Faculty of Engineering
Takeda 4-3-11, Kofu
Yamanashi, Japan

Y. SHIRAI
Osaka University
Faculty of Engineering
Dept. of Mechanical Eng. for
Computer Controlled Machinery
2-1, Yamadaoka
Suitasi, Japan

H. YOSHIKAWA
University of Tokyo
Dept. of Precision Machinery Eng.
Faculty of Engineering
7-3-1 Hongo, Bunkyo-ku
Tokyo, Japan

Special Column Editor

R.R. Murphy
University of South Florida
Dept. of Computer Science and
Engineering
4202 East Fowler Avenue
ENB 118
Tampa, FL 22620-5399, USA.
E-mail: murphy@csee.usf.edu.

Founding Editor

Dr. T.M. Knael
10324 Lake Avenue
Cleveland
OH 44102-1239, USA